Integrated on-board EV battery chargers: New perspectives and challenges for safety improvement

Integrated On-Board EV Battery Chargers: New Perspectives and Challenges for Safety Improvement

Mauro Valente, Thiwanka Wijekoon, Francisco Freijedo
Power Conversion Technology Laboratory
Huawei Technology Duesseldorf GmbH
Nuremberg, Germany
mauro.valente@huawei.com

Paolo Pescetto, Gianmario Pellegrino and Radu Bojoi
Department of Energy
Politecnico di Torino
Turin, Italy
paolo.pescetto@polito.it

***Abstract*—Thanks to the heavy reduction of cost and volume, integrated On-Board Chargers (OBCs) represent an effective solution to provide a versatile and powerful charging system on board of electric and plug-in electric vehicles, combining the charging function with the traction drivetrain. Such integration foresees the use of the traction motor windings as reactive elements and the traction inverter as AC/DC converter. However, this integration brings several challenges on the table. At first, shaft torque production must be avoided to reduce the losses and mechanical stress. A second challenge is to improve the filtering capability of the motor windings in order to meet the grid standards in terms of current distortion and power factor correction. At last, the most critical issue is to meet the safety standards in terms of leakage current, since it represents a risk to human operators and could also hamper the smooth operation of the charger. Therefore, this paper aims at giving a comprehensive review of the challenges in designing integrated chargers. After reviewing the architectures available in literature, an exemplifying structure of integrated OBC will be analysed in terms of leakage current generation and compliance with the relevant standards, along with an introduction to those solutions which use the machine as isolation transformer. Conclusions are given on the prospect for making integrated on-board chargers safer and more reliable.**

***Index Terms*—electrical and hybrid vehicles, integrated battery charger, safety**

I. Introduction

The transportation electrification process is dominated by the fast-growing adoption of Battery powered Electrical Vehicles (BEV) and plug-in Hybrid Electric Vehicles (HEV). On one hand, the battery technology plays a key role in increasing the vehicles autonomy and overcoming the range anxiety of the customers. One the other hand, the battery charging systems have received a lot of attention in the last years to reduce the charging time while preserving the battery lifetime. Battery chargers are divided into on-board chargers (OBC) and off-board chargers. An OBC is an AC/DC converter fed from an AC charging station, as shown in Fig.1 for a BEV. The literature reports many OBC single-phase and three-phase solutions having different power levels that are typically between 3.3 kW and 22 kW [1]. With no exceptions, the OBC needs dedicated input filters to keep the total distortion of the AC input currents at reasonable limits.

As shown in Fig.1, the OBC is a standalone component in a vehicle. Fig.1 includes also the electrical powertrain (ePT) consisting of the traction inverter and the electrical motor, as well as other power electronic converters (DC-DC converters) for auxiliary loads and also to interface the high voltage traction battery with the low voltage (12V) battery. To reduce the number of components and thus the volume and weight, a possible solution is to exploit the ePT not only for traction but also for battery charging to obtain an integrated On-Board Charger (iOBC).

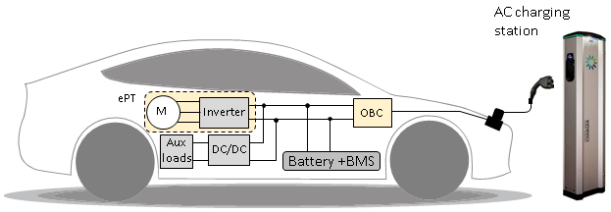

Fig. 1: On-board charger on a BEV.

The dawn of the iOBC dates back to 1985 [2], when a three-phase motor connected to a thyristor-based two-level inverter was proposed to provide charging functions connected to a single-phase grid. Since then, several different developments of the iOBC concept have been proposed in literature, as widely reviewed in [3] and [4].

All the surveys on iOBCs available in the literature focused on the power conversion, i.e. on converter topologies, motor design and control solutions able to charge the battery from the grid without torque production. However, according to the authors' best knowledge, the literature does not include a survey on iOBCs dealing with the critical issues of the safety standards regarding the leakage currents. Therefore, the contribution of this work is to provide a comprehensive overview on iOBCs giving a new perspective with regard to the safety standards against the leakage current and related risks to humans during the charging process.

This paper is organized as follows. A brief classification and a description of the requirements imposed to the iOBC are presented in Section II. The electrical machine modelling and configuration for integrated chargers are described in Section III. The new perspectives on safety using either galvanic insulation provided by the machine or by employing particular

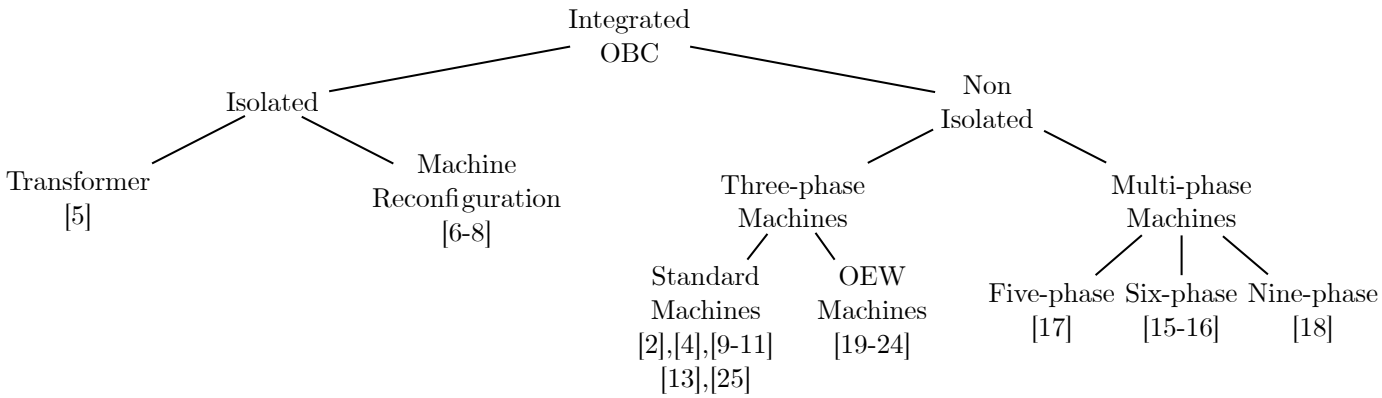

Fig. 2: Classification of integrated On-Board Chargers.

converter solutions for non-isolated iOBC are provided in Section IV, while Section V ends the paper.

II. Classification and Requirements

As emerges from surveys [3], [4], the integrated OBCs can be categorised into isolated and non-isolated, as illustrated in Fig.2. The galvanic isolation can be provided by an additional transformer placed on the low-frequency AC side, as in [5], or by reconfiguring the connections of the electrical machine to make it acting as a transformer. Solutions of this kind have been proposed in [6] and [7], where a six-phase and a nine-phase machines, respectively, are reconfigured to provide galvanic isolation when connecting to a three-phase grid. In [8], a six-phase machine is used as transformer and provides galvanic isolation in both three- and single-phase input operation, with the peculiarity of achieving torque-free charging in single-phase configuration.

On the side of non-isolated integrated OBCs, the classification can be further developed into three-phase and multi-phase machines groups. The solutions built around the three-phase motors can be divided into standard three-phase motors and Open-End Winding Machines (OEWM). The three-phase machine-based group includes single-stage [2], [4], [9], [10] and two-stage OBC solutions [11]–[13]. The single-stage solutions use the motor inductances as an input filter and the inverter as AC/DC converter. Such solutions are more compact respect to the two-stage counterparts. On the other hand, the two-stage solutions employ an additional converter and do not generate torque during charging, since the motor windings are used as DC inductors for the DC-DC stage. A similar distinction can be made for the OEWM configurations. Indeed, single-stage solutions of this kind have been proposed in [14], [15], where a DC fast charger is built using the motor inductances as DC inductors. Additionally, in [15], the system can be configured to provide charging functions under single-phase grids. In [16], the operation of the same architecture is extended to single-phase operation by the addition of an Active Front End (AFE) rectifier; this solution is a two-stage. Lastly, non-isolated integrated chargers have been proposed exploiting the additional degrees of freedom provided by machines with more than three phases to achieve torque-free charging with both single- and three-phase grid. These solutions have been proposed for five-phase [17], six-phase [18]–[20] and nine-phase [21] motors.

With reference to Table I, the machines used in traction applications are mostly Permanent Magnet Synchronous Machines (PMSM) and Induction Machines (IM), thanks to their low weight and high power density [22]–[24]. In most of the applications, the IM machine has a die-cast squirrel cage rotor, which can be either made of aluminium or copper. Although the aluminium is more lightweight, higher power densities are possible with copper. On the other hand, PMSMs have progressively replaced the IMs for their higher compactness and reduced rotor losses, as reported in [25]. Among the different structures of PMSMs, the Interior Permanent Magnet (IPM) structures are normally preferred because of their reluctance torque contribution and constant power speed range capability. A trend towards the reduction or elimination of rare-earth permanent magnet materials from the machine construction is also evident.

TABLE I: Comparative table of the surveyed iOBC solutions.

Ref.	Year	Motor Type	#Motor Phases	#Reconfig. Switches	Stages	Grid Type	No Torque	Isolation
[2]	1985	IM	3	1	1	1-ϕ	Yes	No
[26]	1994	2 IMs	3	1	1	1-ϕ	Yes	No
[10]	1995	4 IMs	3	4	1	1-ϕ	Yes	No
[11]	2009	IPM	3	1	2	1-ϕ	Yes	No
[27]	2010	PMSM	3[a]	0	1	3-ϕ	Yes	No
[6]	2011	IPM	6	0	1	1-,3-ϕ	No	Yes
[13]	2014	PMSM	3	0	2	3-ϕ	Yes	No
[21]	2014	IM	9	0	1	1-,3-ϕ	Yes	No
[17]	2015	IM	5	4	1	1-,3-ϕ	Yes	No
[19]	2016	IM	6	7	1	3-ϕ	Yes	No
[12]	2017	PMSM	3	0	2	3-ϕ	Yes	No
[18]	2017	IM	6	3	1	1-,3-ϕ	Yes	No
[14]	2017	PMSM	3 OEW	2	1	DC	Yes	No
[16]	2018	PMSM	3 OEW	2	2	1-ϕ	Yes	No
[28]	2018	PMSM	3 OEW	2	2	1-ϕ	Yes	No
[4]	2019	SPM	3	3	1	1-ϕ	Yes	No
[29]	2019	PMSM	3 OEW	0	2	3-ϕ	Yes	No
[30]	2019	PMSM	3 OEW	2	2	3-ϕ	Yes	No
[15]	2019	PMSM	3 OEW	2	2	1-ϕ	Yes	No
[8]	2020	IPM	6	3	1	1-,3-ϕ	Yes[b]	Yes

[a] Split-phase.
[b] Only with single-phase grid charging.

A. Requirements for No-torque Production

A common downside of iOBC is the risk of torque production during charging operation. Depending on the adopted

iOBC structure and control, the produced torque can be null, continuous, pulsating at the double of grid frequency or pulsating at high frequency. This might cause mechanical stress to the shaft and bearings, need for rotor locking (in case of a continuous torque) or requiring a disconnecting clutch for separating the motor from the wheels shaft in charging mode. Overall, the iOBC solutions producing shaft torque cause relevant mechanical issues, which often vanish the promises offered by the charger integration.

B. Safety Requirements for Leakage Current

Non-isolated OBCs present a safety issue due to the lack of galvanic isolation. This issue is related to the presence of a leakage current, generated by the common-mode (CM) voltage of the power converter. In the event that a human being touches the vehicle, part of the leakage current flows through the human body, originating a touch current. Such current, if above certain limits, may injure the user. Therefore, international organizations have set limits for the touch current, in order to guarantee safety in the operation of EVs' chargers.

The IEC61851-1 [31] describes the minimum safety requirements for EV chargers with rated supply voltage up to 1 kV. The limits are categorised for Class I and Class II devices, namely devices with standard and double or reinforced insulation, respectively, as described in IEC61140 [32]. Generally, an integrated charging system is of Class I type, due to the high cost of a Class II insulation; therefore the following analysis will be focused on this category of device. The limit of interest is defined as the touch current that flows between any grid pole and metal parts of the vehicle, and it is equal to 3.5 mA for a sinusoidal waveform of frequency equal to 50 Hz [33]. In order to measure such current, a specific circuit is described in IEC60990 and illustrated in Fig.3 . This circuit consists of two networks: a first circuit that emulates the body impedance, cascaded with another one that is frequency sensitive. The need for a frequency sensitive circuit is to emulate the frequency effect on the human body and thus refer any high frequency current to an equivalent low frequency limit. The total circuit has a low-pass filter behaviour, meaning that high-frequency components of the leakage currents are going to be attenuated [34]. Referring to Fig.3, the touch current that flows through the terminals A and B is measured by capturing the voltage V_3, which is related to the touch current by:

$$I_{touch} = \frac{V_3}{500} \tag{1}$$

Lastly, this IEC standard provides limits for the Residual Current Device (RCD). For those devices which do not provide galvanic isolation, the maximum residual current is 30 mA [31].

The limits described by UL2202 [35] are stricter than the ones imposed by IEC61851. The limit for devices that are provided with the PE conductor must have a leakage current under 0.75 mA RMS. An exception is made for devices that are equipped with an EMI filter and a PE conductor, and that the leakage current is more likely to flow through ground rather than through the human body. For those devices that lie in this case, the limit can be increased to 3.5 mA RMS. However, the likelihood that a certain charger configuration lies in this group depends on the grounding system, which can differ among countries. The measurement method outlined by UL2202 is, in principle, similar to the one of IEC61851-1, with the only difference in the frequency sensitive branch, as shown in Fig.3. An overview of the discussed touch current limits and the corresponding voltage measurement are given in Table II.

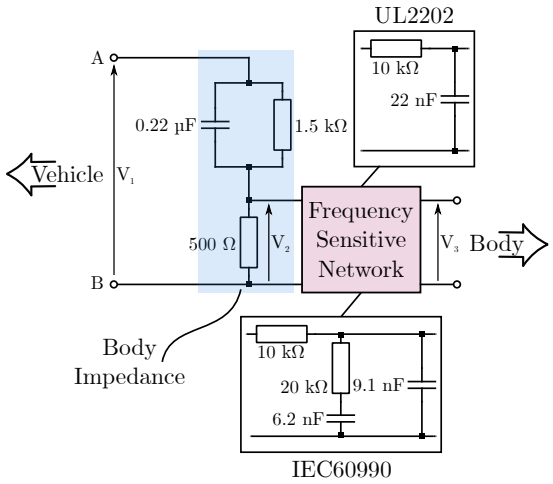

Fig. 3: Circuit diagram for the touch current measurement as prescribed by IEC60990 [33] and UL2202 [35], with the two different frequency sensitive networks.

TABLE II: Summary of the leakage current limits and voltage reading for each standard.

	$\mathbf{I_{touch}}$ **[mA@50Hz]**	$\mathbf{V_3}$**[V]**
IEC61851	3.5 peak	1.75 peak
UL2202	0.75/3.5 RMS[a]	0.375/1.75 RMS[a]

[a]Provided that the charging system configuration fulfils the exception.

III. Electrical Machine Modeling and Configuration

As highlighted in previous Sections, the IPM machine is the preferred choice in traction. A simplified model at standstill is presented here to account for how the machine parameters play and how torque tends to arise in charging mode, as a strict safety requirement during battery charging is torque-free operation. The machine circuital model represented in Fig. 4 is described by the voltage equation:

$$\boldsymbol{v_{abc}} = R_s \boldsymbol{i_{abc}} + \frac{d\boldsymbol{\lambda_{abc}}}{dt} \tag{2}$$

where the phase voltage, current and flux linkage quantities are indicated. R_s is the stator phase resistance. The flux linkage accounts for a leakage and a magnetizing (mutually coupled) component, according to

$$\boldsymbol{\lambda}_{abc} = L_\sigma \boldsymbol{i}_{abc} + \boldsymbol{L_m}\left(\boldsymbol{i_{abc}}, \theta\right) \cdot \boldsymbol{i_{abc}} + \boldsymbol{\lambda_{pm}}\left(\theta\right) \tag{3}$$

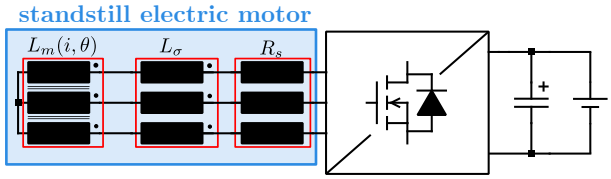

Fig. 4: Simplified model of generic 3-phase drive at standstill.

where $\boldsymbol{\lambda}_{pm}(\theta)$ is the permanent magnet flux linkage. The $\boldsymbol{L_m}$ matrix dependency on the rotor position θ and phase current $\boldsymbol{i}_{abc}$ is expressed in terms of direct and quadrature inductance components.

$$\boldsymbol{L_m} = \frac{L_{md}+L_{mq}}{2}\begin{bmatrix} 1 & -\frac{1}{2} & -\frac{1}{2} \\ -\frac{1}{2} & -\frac{1}{2} & 1 \end{bmatrix} + \ldots$$

$$\ldots + \frac{L_{md}-L_{mq}}{2}\begin{bmatrix} \cos(2\theta) & \cos\left(2\theta-\frac{2\pi}{3}\right) & \cos\left(2\theta+\frac{2\pi}{3}\right) \\ \cos\left(2\theta-\frac{2\pi}{3}\right) & \cos\left(2\theta+\frac{2\pi}{3}\right) & \cos(2\theta) \\ \cos\left(2\theta+\frac{2\pi}{3}\right) & \cos(2\theta) & \cos\left(2\theta-\frac{2\pi}{3}\right) \end{bmatrix} \quad (4)$$

The 3-phase current and flux vectors can be transformed to the dq rotating reference frame, defined in Fig.5, using the Park transformation [36]. The vectors $\boldsymbol{i}_{dq} = [i_d\ i_q]^T$ and $\boldsymbol{\lambda}_{dq} = [\lambda_d\ \lambda_q]^T$ are obtained, respectively. The motor torque can be expressed as:

$$T = \frac{3}{2}p(\boldsymbol{\lambda}_{dq} \wedge \mathbf{i}_{dq}) = \frac{3}{2}p(\lambda_d i_q - \lambda_q i_d) \quad (5)$$

where p is the number of pole pairs.

A. Motor Inductances in Charging Mode

The size of the grid side inductors is crucial in the design of OBCs, influencing many aspects such as the grid current total harmonic distortion (THD), the converter's switching frequency and its control stability. In iOBCs the motor is essentially used as an inductor or as an isolation transformer, although not being magnetically designed for this purpose. Therefore, the resulting inductance may not match the iOBC requirements in terms of rated current value and saturation flux. In this respect, the solutions in the literature can be classified into topologies using the L_σ alone or combined with the $\boldsymbol{L}_m$ terms or a fraction of those. For a properly designed machine L_σ is much lower than any term of $\boldsymbol{L_m}$. Moreover, the typical values of L_σ and $\boldsymbol{L}_m$ strongly depend on the adopted motor type and ratings in terms of nominal speed, torque, DC-bus voltage and number of phases. Finally, in multi-three-phase drives the inductances of $\boldsymbol{L}_m$ mutually couple each stator phase to all the others.

B. Methods for Avoiding Torque During Charging

The capability of avoiding torque production is a key indicator of the feasibility of an iOBC. Considering (5), the possible strategies for avoiding torque production are producing zero stator current in dq reference frame or forcing the vectors $\boldsymbol{\lambda}_{\mathbf{dq}}$ and $\mathbf{i}_{\mathbf{dq}}$ to be parallel.

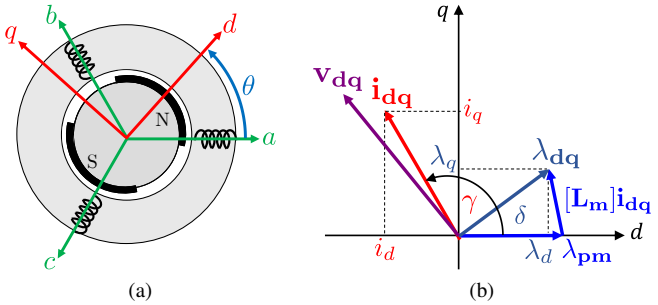

Fig. 5: (a) dq directions definition and (b) vector diagram for PMSM.

A principle often adopted for avoiding torque generation is to excite the machine with a homopolar current only [10], [11], [13], [21], [37]–[41], resulting in $\mathbf{i_{dq}} = 0$. This is applicable for 3-phase motors and single-phase inlet iOBC [11], [13], [37]–[39], for EVs employing multiple motors [10], [41] or for 3-phase inlet, 9-phase motors [21], [40]. In these solutions, the inverter control forces the grid current to equally split in the three phases, thus only creating leakage flux and consequently zero torque is produced, independently from the motor being a PMSM or an IM. This type of techniques are effective, but can give three shortcomings. The first is that possible inaccuracies in the control may cause uneven split of the current in the three stator phases, resulting in a pulsating $\boldsymbol{i_{dq}}$ vector and torque and vibration at the double of the grid frequency in PMSMs. Anyway, with proper inverter control the produced torque is quite small. The second issue is that the machine only introduces L_σ to the PE circuit, which may be too small to be used as boost inductor at charging stage, thus leading to high required switching frequency or excessive grid current THD. This issue can be solved by introducing an additional external inductor [38], but limiting the advantages of the OBC integration, or by adopting dedicated modulation strategies [11]. Finally, it requires access to the star point of the machine, which may not be available.

A second option, suitable for single-phase main inlet, is to exploit a single-phase excitation of the machine [12], [26], [42], [43]. In this case, the grid current flows through one of the three motor phases and then is split among the other two, producing pulsating excitation with fixed spatial direction, and so pulsating $\boldsymbol{i_{dq}}$ and $\boldsymbol{\lambda_{dq}}$ vectors. If the adopted machine is an IM [26], torque is not produced thanks to its isotropic nature. Conversely, for EVs adopting PMSMs [12], [43] a relevant torque is produced, compatible with the rated torque, unless a dedicated initial mechanical alignment of the rotor is provided. With a proper rotor alignment, $\boldsymbol{i_{dq}}$ can be forced to be parallel to $\boldsymbol{\lambda_{dq}}$, thus not producing torque. Anyway, foreseeing a mechanical alignment of the rotor can be a relevant issue for EVs. Moreover, also in this case if the alignment is not sufficiently accurate, a pulsating torque at twice the grid frequency will be produced. Since such torque component is related to the mechanical position, it is normally more difficult to control or cancel it with respect to the solutions in [11],

[37], [38]. On the other hand, in these topologies the machine introduces its full magnetizing inductance to the circuit, thus simplifying the current filtering and boost control even at limited switching frequency.

Some of the proposed topologies [6], [44]–[46] excite the machine with a magnetic field rotating at grid frequency. The resulting torque depends on the motor type. For IMs, a strong continuous torque is produced, thus requiring mechanical rotor locking. Moreover, depending on the IM ratings the input magnetizing current may be very high. For PMSMs, if the rotor is locked to avoid rotation, as in [45], a relevant pulsating torque is produced, with unacceptable mechanical stress on the shaft and bearings. To solve this issue, [6], [44], [46] proposed to charge the EV with the motor continuously rotating at free-shaft, mechanically disconnected from the wheels. This solution is interesting, but leads to significantly complex mechanical arrangement, friction losses and bearings consumption during charging.

Recently, the adoption of multiphase machines, already popular in high power high current applications, is becoming appealing also for EVs. When used in iOBCs the additional degrees of freedom with respect to standard 3-phase machines permit a wider number of options for avoiding torque production. As an example, [47] reviews a series of solutions where the windings are properly rearranged to excite the machine in its homopolar planes, thus not producing torque. Unfortunately, some of these topologies, e.g. [48] are designed for multiphase main inlet, so they require dedicated off-board transformers. For other topologies [49], despite designed for 3-phase input, an external transformer is still required for providing galvanic insulation. A different approach was proposed in [8], [50], where dedicated control strategies were developed to achieve zero torque and low grid current THD, at unitary PF. The adopted principle is to force the current vector i_{dq} to be parallel to the flux vector λ_{dq}, while its amplitude is determined by the required grid current.

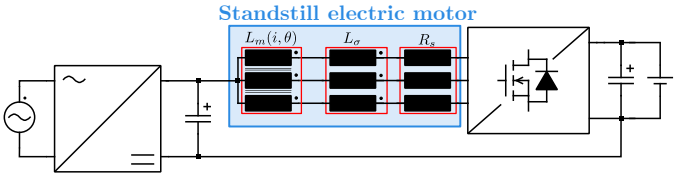

Fig. 6: Example of torque-free integrated charger. [11]

IV. New Perspectives on Safety

It has been outlined that the main concerns in designing iOBCs are related to the leakage current generation during charging operations. In traditional stand-alone OBCs, the leakage current is limited by the galvanic isolation and different CM filter structures. To improve the feasibility of non-isolated iOBCs, reducing the leakage current to the levels given in Sec. II-B is a viable option [34]. On the other hand, the machine windings may be rearranged to form a low-frequency transformer to isolate the grid from the charging stage. This section is devoted to provide perspectives from both point of views.

A. Non-Isolated Solutions

It has been outlined that the main limitation in using non-isolated charging solution is the generation of leakage current, dangerous for human beings and neighbour devices. Moreover, the ground current must be kept under 30mA, as prescribed in [31], to avoid tripping of the RCD. In summary, a proper functioning non-isolated iOBC must comply with the standards from both touch and ground current limits viewpoint. In literature the issue has been addressed and a detailed modelling has been provided [34]. A key aspect to be considered is the structure of the grounding system. Among the grounding concepts described in IEC60364, there are two type of grounding systems which are common to charging applications, namely TT and TN [51]. As underlined in [34], the solution that leads to a higher leakage current is the TT, since the grounding is provided locally with an impedance higher than the PE as provided in the TN configuration.

To understand the interaction between the OBC, the grounding system and the possible human interaction, a simplified model is needed. Such model has been provided in [34] and is reported in Fig.7 including the additional parasitic couplings within the motor, the converter and the battery. As shown in Fig.7, the battery is coupled with the car chassis through its insulating layer and such capacitance can reach high value when the interface between the battery and the chassis is large [52], as in most of the cases. The capacitive couplings within the motor are created between the windings and the enclosure, and between the windings and the rotor [53], [54]. Besides these additional couplings, the CM filters, required to comply with IEC61851-21 [55], play a vital role. In particular, the large Y-capacitor capacitors on the DC-Link side generate high leakage current due to the CM voltage generated by the switching action of the power converter [34]. Overall, the system illustrated in Fig.7 has a low-pass filter behaviour, with resonance peaks at specific frequencies, which depend on the system parameters.

The leakage current is, as known, generated by CM voltage generated by the switching action of the power converter. [54], [56]. In a general form, the CM voltage can be expressed as [57]:

$$V_{CM} = \frac{1}{N}\sum_{n=1}^{N} v_{nO} \tag{6}$$

where N is the total number of phases and v_{nO} is the voltage between the phase output and the reference point, usually identified as the mid-point of the DC-Link. Assuming a two-level three-phase inverter, modulated with the sinusoidal PWM strategy (Sine-PWM), the CM voltage can assume values equal to $\pm V_{DC}/2$ and $\pm V_{DC}/6$ with a fundamental frequency equal to the switching frequency [58]. The dv/dt transitions of the CM, which are equal to the dv/dt of the converter's transistors, are responsible for the generation of high current spikes in the CM path and ultimately in the

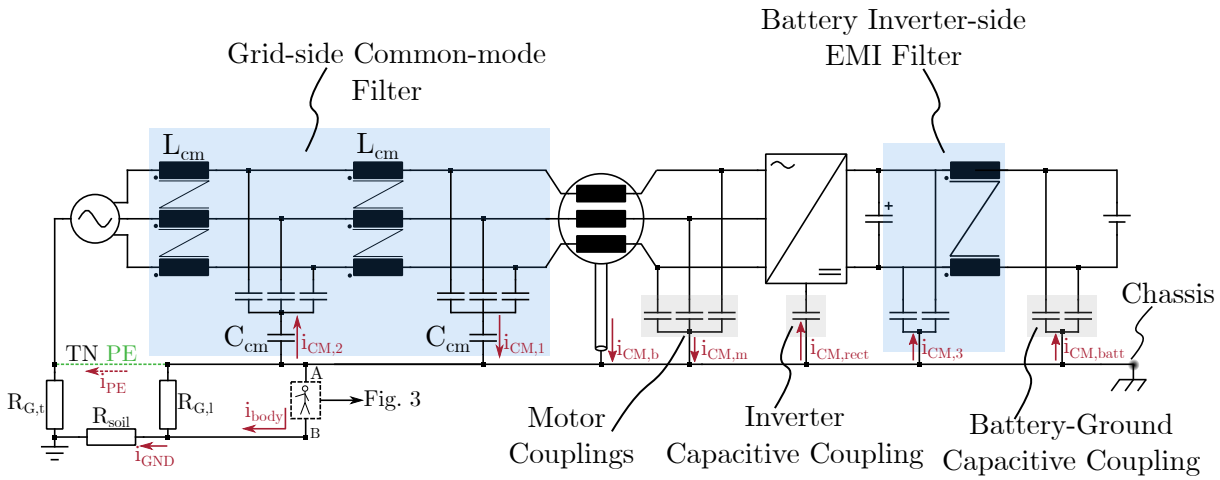

Fig. 7: Conceptual schematic of the integrated OBC, including the parasitic capacitances, EMI filters and the ground connections. The two possible ground configurations are included, where i_{PE} indicates the current path in TN grid and i_{GND} in TT grid.

leakage current. With the advent of modern Wide Band-Gap devices (WBG), such dv/dt slopes are getting larger in order to allow an increase in switching frequency. Thus, if on one hand the higher the switching frequency the lower the risk on the user, the steep voltage transients may induce high leakage currents anyway. The switching frequency component of the CM voltage is responsible for the higher part of the leakage current. As demonstrated in [34] and [52], a switching frequency of 10 kHz with a two-level inverter with Sine-PWM leads to leakage currents that surpass the limits. Therefore, a possible reduction of the leakage current can be found in the increase of the switching frequency. Another aspect that needs to be considered is the situations in which the filtering inductances are not balanced. As mentioned in [59], an unbalance in the inductances leads to the addition of a low-frequency component on the CM voltage. Therefore, in such a case, the low-frequency component of the leakage current may reach significant values and increase the risk of electric shock for the user.

At this point, it results clearly that the CM voltage should be ideally constant, or at least with reduced voltage amplitude and at high frequency. In the panorama of two-level inverter modulations, a class of modulation techniques called Reduced CMV PWM (RCMV-PWM) comprises several modulation techniques that aims to reduce the CMV. The authors of [58] have extensively reviewed the performances of these techniques. Discarding the modulations that have implementation difficulties or poor performances, the best performing modulation is the Near State PWM (NSPWM) [60], which produces a CM voltage at twice the switching frequency and amplitude reduced to $\pm V_{DC}/6$. However, if the dead-time is considered, the CM voltage would present spikes up to $\pm V_{DC}/2$ during the simultaneous transitions. In [61], this problems are addressed and a compensation method is proposed to suppress the dead-time effect, leading to a CM voltage as in the ideal case.

Another possibility of reducing the CM voltage amplitude, is offered by multi-level inverters. As outlined in [62], [63], the three-level inverters are seen with favour from the automotive industry, thanks to the lower voltage-class devices required, superior harmonic distortion performances and reduced CM voltage. With traditional Space Vector Modulation (SVM), the CM voltage of a three-level inverter fluctuates six times in a switching period and it assumes peak values of $\pm V_{DC}/3$. However, with specific modulations as described in [64], zero CM voltage can be achieved if the dead-time is not considered. The effect of the dead-time can be effectively eliminated as proposed in [65].

Besides the possibilities offered by different modulation techniques and topologies, the leakage current can be reduced by means of different filtering such as active EMI filter [66] and floating filters [67]. The floating filter has proven to be effective in reduction of the total leakage current, but no information on the touch current level is given.

TABLE III: Common-mode voltage reduction modulations for two- and three-level NPC inverters.

		$\mathbf{V_{CM,max}}$	**f**
2L	SVM	$\pm V_{DC}/2$	f_{sw}
	NSPWM	$\pm V_{DC}/2$	$2f_{sw}$
	NSPWM dead-time comp.	$\pm V_{DC}/6$	$2f_{sw}$
3L	SVM	$\pm V_{DC}/3$	f_{sw}
	ZCMV	$\pm V_{DC}/3$	$3f_{fund}$
	ZCMV dead-time comp.	0	DC

B. Galvanic Isolation Using the Machine

An effective solution for reducing leakage currents during charging is isolating the battery with respect to the grid inlet. This is normally done in stand-alone OBCs by using HF isolation transformers, but galvanic isolation is not provided by most of the iOBCs, with few exceptions. To meet the concepts of integration and isolation, a feasible option is to exploit the machine itself as an isolation transformer at grid frequency. It should be noted that, in this case, the grid voltage amplitude

v_g and frequency f_g impose the amplitude of the flux linkage λ_g in the grid connected windings. Assuming a 230V, 50 Hz grid:

$$\hat{\lambda}_g = \frac{\hat{v}_g}{2\pi f_g} \approx 1Vs \tag{7}$$

Such flux linkage is much higher than the rated flux of most of

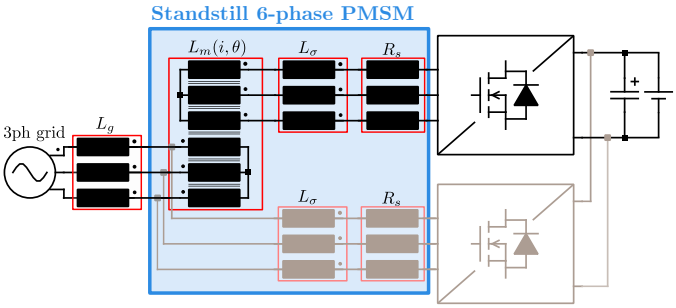

Fig. 8: 6-phase e-drive used as isolation transformer.

the EV traction motors, normally designed for medium-high speed operation to achieve high power density and efficiency. It should be remarked that the higher is the rated speed of the motor, the lower is its rated flux.

An example of isolated iOBC is given in [68], adopting a wound field IM. In charging mode, the stator windings are connected to the phase grid inlet, while the rotor winding are inverter controlled to regulate the grid current and battery charging. Despite galvanic isolation is effectively provided, wound field IMs are seldom adopted in EVs due to their complex manufacturing and need of rotating contacts, which ultimately require additional maintenance. A different approach was adopted in [44], proposing a PMSM with a custom designed stator winding. A standard 3-phase winding is used for traction, while a second additional winding is insert in the same slots and grid connected at charging stage, to form the isolation transformer. Despite galvanic isolation is obtained, the machine design stage is complicated, and the power density and compactness of the drive in traction mode are necessarily reduced, since the slots have to host a second 3-phase set not adopted for traction. A similar topology was presented in [6], where the 3-phase winding is split in two parts in charging mode by accessing the mid point of each winding. In this case, one part of the winding is connected to the grid and the other one to the inverter. The motor power density in traction mode is not significantly affected, but still the required reconfiguration is quite complex, including access to the mid-point of the windings. Moreover, half of the stator winding has to sustain the full grid voltage at grid frequency, which means the grid excitation flux (7) is linked with only half of the stator turns. This may cause very deep magnetic saturation of the machine. Moreover, [6], [44] require machine disconnection at charging stage, to rotate at free-shaft, thus adding mechanical issues. Another solution is proposed in [8], [50] adopting a six phase machine, where, in charging mode, one of the two three-phase sets is connected to the grid. In this case, the required reconfiguration is simpler, and λ_g is linked with the full stator winding, thus halving the saturation requirements with respect to [6]. Moreover, the charging is performed at standstill.

V. Conclusion

Although promising from the power density point of view, integrated OBCs still present challenges in their implementation, especially from the safety perspective. Indeed, the safety requirements for the touch current, prescribed by the standards IEC61851 and UL2202, are strict. In the framework of a high degree of system integration, the use of additional components has to be avoided, including transformers to provide galvanic isolation. From this viewpoint, this paper has reviewed different means to comply with the safety standards: 1) reducing the leakage current by acting on the converter and filtering, and 2) configuring the electrical machine as line-frequency transformer. Thus, if with the first method a three-phase motor combined with proper converter topology and modulation may be sufficient, the second one requires a multi-phase machine design optimised to operate as line-frequency transformer.

References

[1] M. Yilmaz *et al.*, "Review of battery charger topologies, charging power levels, and infrastructure for plug-in electric and hybrid vehicles," 2151–2169 28 *IEEE transactions on Power Electronics*, 2012.

[2] D. Thimmesch, "An scr inverter with an integral battery charger for electric vehicles," 1023–1029 *IEEE Trans. Ind. Appl.*, 1985.

[3] M. Y. Metwly *et al.*, " 85216–85242 8 "A review of integrated on–board ev battery chargers: Advanced topologies, recent developments and optimal selection of fscw slot/pole combination, 2020.

[4] T. Na *et al.*, "A review of on-board integrated electric vehicles charger and a new single-phase integrated charger," 288–298 4 *CPSS Transactions on Power Electronics and Applications*, 2019.

[5] I. Subotic *et al.*, "Isolated chargers for evs incorporating six-phase machines," 653–664 63 *IEEE Trans. Ind. Electron.*, 2015.

[6] S. Haghbin *et al.*, "An isolated high-power integrated charger in electrified-vehicle applications," 4115–4126 60 *IEEE Trans. Veh. Technol.*, 2011.

[7] A. S. Abdel-Khalik *et al.*, "Interior permanent magnet motor-based isolated on-board integrated battery charger for electric vehicles," 124–134 12 *IET Electr. Power Appl.*, 2017.

[8] P. Pescetto *et al.*, "Integrated isolated obc for evs with 6-phase traction motor drives," in *2020 IEEE Energy Conversion Congress and Exposition (ECCE)*. 4112–4117 IEEE, 2020.

[9] W. E. Rippel *et al.*, "Integrated motor drive and recharge system," Mar. 24 1992, uS Patent 5,099,186.

[10] S.-K. Sul *et al.*, "An integral battery charger for four-wheel drive electric vehicle," 1096–1099 31 *IEEE Trans. Ind. Appl.*, 1995.

[11] G. Pellegrino *et al.*, "An integral battery charger with power factor correction for electric scooter," 751–759 25 *IEEE transactions on power electronics*, 2009.

[12] C. Shi *et al.*, "A three-phase integrated onboard charger for plug-in electric vehicles," 4716–4725 33 *IEEE Trans. Power Electron.*, 2017.

[13] S. Loudot *et al.*, "Fast charging device for an electric vehicle," Sep. 30 2014, uS Patent 8,847,555.

[14] R. Shi *et al.*, "Constant current fast charging of electric vehicles via a dc grid using a dual-inverter drive," 6940–6949 64 *IEEE Trans. Ind. Electron.*, 2017.

[15] S. Foti *et al.*, "An integrated battery charger for ev applications based on an open end winding multilevel converter configuration," in *2019 21st European Conference on Power Electronics and Applications (EPE'19 ECCE Europe)*. P–1 IEEE, 2019.

[16] S. Semsar *et al.*, "Integrated single-phase electric vehicle charging using a dual-inverter drive," in *2018 IEEE Transportation Electrification Conference and Expo (ITEC)*. 320–325 IEEE, 2018.

[17] I. Subotic *et al.*, "An ev drive-train with integrated fast charging capability," 1461–1471 31 *IEEE Trans. Power Electron.*, 2015.

[18] I. Subotic *et al.*, "Integration of six-phase ev drivetrains into battery charging process with direct grid connection," 1012–1022 32 *IEEE Trans. Energy Convers.*, 2017.

[19] M. S. Diab *et al.*, "A nine-switch-converter-based integrated motor drive and battery charger system for evs using symmetrical six-phase machines," 5326–5335 63 *IEEE Trans. Ind. Electron.*, 2016.

[20] L. De Sousa *et al.*, "Method and electric combined device for powering and charging with compensation means," Oct. 6 2015, uS Patent 9,153,996.

[21] I. Subotic *et al.*, "Onboard integrated battery charger for evs using an asymmetrical nine-phase machine," 3285–3295 62 *IEEE Transactions on industrial electronics*, 2014.

[22] E. Agamloh *et al.*, "An overview of electric machine trends in modern electric vehicles," 20 8 *Machines*, 2020.

[23] A. M. El-Refaie, "Motors/generators for traction/propulsion applications: A review," 90–99 8 *IEEE Veh. Technol. Mag.*, 2013.

[24] Z.-Q. Zhu *et al.*, "Electrical machines and drives for electric, hybrid, and fuel cell vehicles," 746–765 95 *Proc. IEEE*, 2007.

[25] L. Shao *et al.*, " 116900–116913 8 "Design approaches and control strategies for energy–efficient electric machines for electric vehicles—a review, 2020.

[26] A. G. Cocconi, "Combined motor drive and battery recharge system," Aug. 23 1994, uS Patent 5,341,075.

[27] L. De Sousa *et al.*, "A combined multiphase electric drive and fast battery charger for electric vehicles," in *2010 IEEE Vehicle Power and Propulsion Conference*. 1–6 IEEE, 2010.

[28] T. Soong *et al.*, "On-board single-phase electric vehicle charger with active front end," in *2018 International Power Electronics Conference (IPEC-Niigata 2018-ECCE Asia)*. 3203–3208 IEEE, 2018.

[29] V. F. Pires *et al.*, "Integrated battery charger for electric vehicles based on a dual-inverter drive and a three-phase current rectifier," 1199 8 *Electronics*, 2019.

[30] S. Wang *et al.*, "Design and control of 3-phase integrated charger for dual-inverter drivetrain electric vehicles," in *2019 IEEE Transportation Electrification Conference and Expo (ITEC)*. 1–6 IEEE, 2019.

[31] I. E. Commission, "Iec 61851-1 - electric vehicle conductive charging system - part 1: General requirements," 2017.

[32] I. E. Commission, "Iec 61140 - protection against electric shock - common aspects for installation and equipment," 2016.

[33] I. E. Commission, "Iec 60990 - methods of measurement of touch current and protective conductor current," 2016.

[34] Y. Zhang *et al.*, "Leakage current issue of non-isolated integrated chargers for electric vehicles," in *2018 IEEE Energy Conversion Congress and Exposition (ECCE)*. 1221–1227 IEEE, 2018.

[35] U. Laboratories, "Ul2202 - standard for electric vehicle (ev) charging system equipment," 2009.

[36] S. K. Sul, *Control of Electric Machine Drive Systems*. Wiley IEEE Press, 2010.

[37] L. Solero, "Nonconventional on-board charger for electric vehicle propulsion batteries," 144-149 50 *IEEE Trans. Veh. Technol.*, Jan 2001.

[38] W. E. Rippel, "Integrated traction inverter and battery charger apparatus," 1990, uS Patent 4 920 475.

[39] Y. Xiao *et al.*, "An integrated on-board ev charger with safe charging operation for three-phase ipm motor," 7551-7560 66 *IEEE Trans. Ind. Electron.*, Oct 2019.

[40] N. Bodo *et al.*, "Efficiency evaluation of fully integrated on-board ev battery chargers with nine-phase machines," 257-266 32 *IEEE Trans. Energy Convers.*, March 2017.

[41] Lixin Tang *et al.*, "A low-cost, digitally-controlled charger for plug-in hybrid electric vehicles," in *2009 IEEE Energy Conversion Congress and Exposition*, 3923-3929 2009.

[42] Lisheng Shi *et al.*, "Single-phase bidirectional ac-dc converters for plug-in hybrid electric vehicle applications," in *2008 IEEE Vehicle Power and Propulsion Conference*, 1-5 2008.

[43] C. Shi *et al.*, "A single-phase integrated onboard battery charger using propulsion system for plug-in electric vehicles," 10899-10910 66 *IEEE Trans. Veh. Technol.*, Dec 2017.

[44] S. Haghbin *et al.*, "Integrated chargers for ev's and phev's: examples and new solutions," in *The XIX International Conference on Electrical Machines - ICEM 2010*, 1-6 2010.

[45] S. Q. Ali *et al.*, "Three phase high power integrated battery charger for plugin electric vehicles," in *2015 IEEE Vehicle Power and Propulsion Conference (VPPC)*, 1-6 2015.

[46] S. Haghbin *et al.*, "An integrated charger for plug-in hybrid electric vehicles based on a special interior permanent magnet motor," in *2010 IEEE Vehicle Power and Propulsion Conference*, 1-6 2010.

[47] V. Katic *et al.*, "Overview of fast on-board integrated battery chargers for electric vehicles based on multiphase machines and power electronics," 10 *IET Electr. Power Appl.*, 03 2016.

[48] I. Subotic *et al.*, "An integrated battery charger for evs based on an asymmetrical six-phase machine," in *IECON 2013 - 39th Annual Conference of the IEEE Industrial Electronics Society*, 7244-7249 2013.

[49] I. Subotic *et al.*, "An integrated battery charger for evs based on a symmetrical six-phase machine," in *2014 IEEE 23rd International Symposium on Industrial Electronics (ISIE)*, 2074-2079 2014.

[50] P. Pescetto *et al.*, "Isolated on-board battery charger integrated with 6-phase traction drive," in *2020 23rd International Conference on Electrical Machines and Systems (ICEMS)*, 309-314 2020.

[51] I. E. Commission, "Iec 60364-1 - low-voltage electrical installations - part 1: Fundamental principles, assessment of general characteristics, definitions," 2005.

[52] S. Liu *et al.*, "An integrated on-board charger with direct grid connection for battery electrical vehicle," in *International Symposium on Power Electronics Power Electronics, Electrical Drives, Automation and Motion*. 335–340 IEEE, 2012.

[53] T. Hadden *et al.*, "A review of shaft voltages and bearing currents in ev and hev motors," in *IECON 2016-42nd Annual Conference of the IEEE Industrial Electronics Society*. 1578–1583 IEEE, 2016.

[54] J. Luszcz, *High Frequency Conducted Emission in AC Motor Drives Fed By Frequency Converters: Sources and Propagation Paths*. John Wiley & Sons, 2018.

[55] I. E. Commission, "Iec 61851-21 - electric vehicle on-board charger emc requirements for conductive connection to ac/dc supply," 2017.

[56] G. L. Skibinski *et al.*, "Emi emissions of modern pwm ac drives," 47–80 5 *IEEE Ind. Appl. Mag.*, 1999.

[57] A. Brovont *et al.*, "Equivalent circuits for common-mode analysis of naval power systems," in *2015 IEEE Electric Ship Technologies Symposium (ESTS)*. 245–250 IEEE, 2015.

[58] A. M. Hava *et al.*, "Performance analysis of reduced common-mode voltage pwm methods and comparison with standard pwm methods for three-phase voltage-source inverters," 241–252 24 *IEEE Trans. Power Electron.*, 2009.

[59] T. Kerekes *et al.*, "Evaluation of three-phase transformerless photovoltaic inverter topologies," 2202–2211 24 *IEEE transactions on Power Electronics*, 2009.

[60] E. Un *et al.*, "A near-state pwm method with reduced switching losses and reduced common-mode voltage for three-phase voltage source inverters," 782–793 45 *IEEE Trans. Ind. Appl.*, 2009.

[61] Y.-S. Lai *et al.*, "Optimal common-mode voltage reduction pwm technique for inverter control with consideration of the dead-time effects-part i: basic development," 1605–1612 40 *IEEE Trans. Ind. Appl.*, 2004.

[62] S. Chowdhury *et al.*, "Enabling technologies for compact integrated electric drives for automotive traction applications," in *2019 IEEE Transportation Electrification Conference and Expo (ITEC)*. 1–8 IEEE, 2019.

[63] J. Reimers *et al.*, "Automotive traction inverters: Current status and future trends," 3337–3350 68 *IEEE Trans. Veh. Technol.*, 2019.

[64] L. Kai *et al.*, "Performance analysis of zero common-mode voltage pulse-width modulation techniques for three-level neutral point clamped inverters," 2654–2664 9 *IET Power Electron.*, 2016.

[65] X. Zhang *et al.*, "Improved common-mode voltage elimination modulation with dead-time compensation for three-level neutral-point-clamped three-phase inverters," in *2013 IEEE Energy Conversion Congress and Exposition*. 4240–4246 IEEE, 2013.

[66] S. Wang *et al.*, "Investigation of hybrid emi filters for common-mode emi suppression in a motor drive system," 1034–1045 25 *IEEE Trans. Power Electron.*, 2009.

[67] Y. Zhang *et al.*, "Leakage current mitigation of non-isolated integrated chargers for electric vehicles," in *2019 IEEE Energy Conversion Congress and Exposition (ECCE)*. 1195–1201 IEEE.

[68] F. Lacressonniere *et al.*, "Converter used as a battery charger and a motor speed controller in an industrial truck," in *2005 European Conference on Power Electronics and Applications*, 7 pp.-P.7 2005.